Acknowledgments

This work was supported by grants to J-IS from Research on Psychiatric and Neurological Diseases and Mental Health, the Ministry of Health, Labour and Welfare of Japan (H17-020), Research on Health Sciences Focusing on Drug Innovation, the Japan Health Sciences Foundation (KH21101), the Grant-in-Aid for Scientific Research, the Ministry of Education, Culture, Sports, Science and Technology, Japan (MEXT) (B18300118), the High-Tech Research Center Project, MEXT (S0801043) and from the Nakatomi Foundation.

References

1. Lassmann, H, Brück, W, Lucchinetti, CF. The immunopathology of multiple sclerosis: an overview. *Brain Pathol* 2007; **17**: 210–218.
2. Kieseier, BC, Wiendl, H, Hemmer, B, Hartung, HP. Treatment and treatment trials in multiple sclerosis. *Curr Opin Neurol* 2007; **20**: 286–293.
3. Kingsmore, SF, Lindquist, IE, Mudge, J, Gessler, DD, Beavis, WD. Genome-wide association studies: progress and potential for drug discovery and development. *Nat Rev Drug Discov* 2008; **7**: 221–230.
4. Steinman, L, Zamvil, S. Transcriptional analysis of targets in multiple sclerosis. *Nat Rev Immunol* 2003; **3**: 483–492.
5. Quintana, FJ, Farez, MF, Weiner, HL. Systems biology approaches for the study of multiple sclerosis. *J Cell Mol Med* 2008; doi 10.1111/j.1582-4934.2008.00375.x.
6. Lock, C, Hermans, G, Pedotti, R, *et al.* Gene-microarray analysis of multiple sclerosis lesions yields new targets validated in autoimmune encephalomyelitis. *Nat Med* 2002; **8**: 500–508.
7. Satoh, J, Nakanishi, M, Koike, F, *et al.* Microarray analysis identifies an aberrant expression of apoptosis and DNA damage-regulatory genes in multiple sclerosis. *Neurobiol Dis* 2005; **18**: 537–550.
8. Han, MH, Hwang, SI, Roy, DB, *et al.* Proteomic analysis of active multiple sclerosis lesions reveals therapeutic targets. *Nature* 2008; **451**: 1076–1081.
9. Ganter, B, Giroux, CN. Emerging applications of network and pathway analysis in drug discovery and development. *Curr Opin Drug Discov Devel* 2008; **11**: 86–94.
10. Viswanathan, GA, Seto, J, Patil, S, Nudelman, G, Sealfon, SC. Getting started in biological pathway construction and analysis. *PLoS Comput Biol* 2008; **4**: e16.
11. Albert, R, Jeong, H, Barabasi, AL. Error and attack tolerance of complex networks. *Nature* 2000; **406**: 378–382.
12. Kanehisa, M, Araki, M, Goto, S, *et al.* KEGG for linking genomes to life and the environment. *Nucleic Acids Res* 2008; **36**: D480–D484.
13. Mi, H, Guo, N, Kejariwal, A, Thomas, PD. PANTHER version 6: protein sequence and function evolution data with expanded representation of biological pathways. *Nucleic Acids Res* 2007; **35**: D247–D252.
14. Palacios, R, Goni, J, Martinez-Forero, I, *et al.* A network analysis of the human T-cell activation gene network identifies JAGGED1 as a therapeutic target for autoimmune diseases. *PLoS ONE* 2007; **2**: e1222.
15. Sato, H, Ishida, S, Toda, K, *et al.* New approaches to mechanism analysis for drug discovery using DNA microarray data combined with KeyMolnet. *Curr Drug Discov Technol* 2005; **2**: 89–98.
16. Luo, BH, Carman, CV, Springer, TA. Structural basis of integrin regulation and signaling. *Annu Rev Immunol* 2007; **25**: 619–647.
17. Sobel, RA. The extracellular matrix in multiple sclerosis lesions. *J Neuropathol Exp Neurol* 1998; **57**: 205–217.
18. van Horssen, J, Dijkstra, CD, de Vries, HE. The extracellular matrix in multiple sclerosis pathology. *J Neurochem* 2007; **103**: 1293–1301.
19. Sobel, RA, Chen, M, Maeda, A, Hinojoza, JR. Vitronectin and integrin vitronectin receptor localization in multiple sclerosis lesions. *J Neuropathol Exp Neurol* 1995; **54**: 202–213.
20. Minagar, A, Jy, W, Jimenez, JJ, *et al.* Elevated plasma endothelial microparticles in multiple sclerosis. *Neurology* 2001; **56**: 1319–1324.
21. Milner, R, Huang, X, Wu, J, *et al.* Distinct roles for astrocyte αvβ5 and αvβ8 integrins in adhesion and migration. *J Cell Sci* 1999; **112**: 4271–4279.
22. Sobel, RA, Mitchell, ME. Fibronectin in multiple sclerosis lesions. *Am J Pathol* 1989; **135**: 161–168.
23. Sisková, Z, Baron, W, de Vries, H, Hoekstra, D. Fibronectin impedes "myelin" sheet-directed flow in oligodendrocytes: a role for a beta 1 integrin-mediated PKC signaling pathway in vesicular trafficking. *Mol Cell Neurosci* 2006; **33**: 150–159.
24. Milner, R, Crocker, SJ, Hung, S, Wang, X, Frausto, RF, del Zoppo, GJ. Fibronectin- and vitronectin-induced microglial activation and matrix metalloproteinase-9 expression is mediated by integrins $\alpha_5\beta_1$ and $\alpha_v\beta_5$. *J Immunol* 2007; **178**: 8158–8167.
25. Ren, Y, Savill, J. Proinflammatory cytokines potentiate thrombospondin-mediated phagocytosis of neutrophils undergoing apoptosis. *J Immunol* 1995; **154**: 2366–2374.
26. Chabas, D, Baranzini, SE, Mitchell, D, *et al.* The influence of the proinflammatory cytokine, osteopontin, on autoimmune demyelinating disease. *Science* 2001; **294**: 1731–1735.
27. Sinclair, C, Kirk, J, Herron, B, Fitzgerald, U, McQuaid, S. Absence of aquaporin-4 expression in lesions of neuromyelitis optica but increased expression in multiple sclerosis lesions and normal-appearing white matter. *Acta Neuropathol* 2007; **113**: 187–194.
28. Vogt, MH, Lopatinskaya, L, Smits, M, Polman, CH, Nagelkerken, L. Elevated osteopontin levels in active relapsing-remitting multiple sclerosis. *Ann Neurol* 2003; **53**: 819–822.
29. Liu, TJ, LaFortune, T, Honda, T, *et al.* Inhibition of both focal adhesion kinase and insulin-like growth factor-I receptor kinase suppresses glioma proliferation *in vitro* and *in vivo*. *Mol Cancer Ther* 2007; **6**: 1357–1367.
30. Swenson, S, Costa, F, Minea, R, *et al.* Intravenous liposomal delivery of the snake venom disintegrin contortrostatin limits breast cancer progression. *Mol Cancer Ther* 2004; **3**: 499–511.
31. Cantor, JM, Ginsberg, MH, Rose, DM. Integrin-associated proteins as potential therapeutic targets. *Immunol Rev* 2008; **223**: 236–251.
32. Steinman, L. Blocking adhesion molecules as therapy for multiple sclerosis: natalizumab. *Nat Rev Drug Discov* 2005; **4**: 510–518.

Cell Mol Neurobiol (2009) 29:423–438
DOI 10.1007/s10571-008-9338-2

ORIGINAL PAPER

Gene Expression Profiling of Human Neural Progenitor Cells Following the Serum-Induced Astrocyte Differentiation

Shinya Obayashi · Hiroko Tabunoki · Seung U. Kim · Jun-ichi Satoh

Received: 16 August 2008 / Accepted: 10 December 2008 / Published online: 7 January 2009

Abstract Neural stem cells (NSC) with self-renewal and multipotent properties could provide an ideal cell source for transplantation to treat spinal cord injury, stroke, and neurodegenerative diseases. However, the majority of transplanted NSC and neural progenitor cells (NPC) differentiate into astrocytes in vivo under pathological environments in the central nervous system, which potentially cause reactive gliosis. Because the serum is a potent inducer of astrocyte differentiation of rodent NPC in culture, we studied the effect of the serum on gene expression profile of cultured human NPC to identify the gene signature of astrocyte differentiation of human NPC. Human NPC spheres maintained in the serum-free culture medium were exposed to 10% fetal bovine serum (FBS) for 72 h, and processed for analyzing on a Whole Human Genome Microarray of 41,000 genes, and the microarray data were validated by real-time RT-PCR. The serum elevated the levels of expression of 45 genes, including ID1, ID2, ID3, CTGF, TGFA, METRN, GFAP, CRYAB and CSPG3, whereas it reduced the expression of 23 genes, such as DLL1, DLL3, PDGFRA, SOX4, CSPG4, GAS1 and HES5. Thus, the serum-induced astrocyte differentiation of human NPC is characterized by a counteraction of ID family genes on Delta family genes. Coimmunoprecipitation analysis identified ID1 as a direct binding partner of a proneural basic helix-loop-helix (bHLH) transcription factor MASH1. Luciferase assay indicated that activation of the DLL1 promoter by MASH1 was counteracted by ID1. Bone morphogenetic protein 4 (BMP4) elevated the levels of ID1 and GFAP expression in NPC under the serum-free culture conditions. Because the serum contains BMP4, these results suggest that the serum factor(s), most probably BMP4, induces astrocyte differentiation by upregulating the expression of ID family genes that repress the proneural bHLH protein-mediated Delta expression in human NPC.

Keywords Astrocytes · Delta family genes · Human neuronal progenitor cells · ID family genes · Microarray

Abbreviations

NSC	Neural stem cells
NPC	Neural progenitor cells
CNS	Central nervous system
BBB	Blood–brain barrier
bHLH	Basic helix-loop-helix
FBS	Fetal bovine serum
EGF	Epidermal growth factor
bFGF	Basic fibroblast growth factor
LIF	Leukemia inhibitory factor
TGF	Transforming growth factor
RT-PCR	Reverse transcription-polymerase chain reaction
DAVID	Database for annotation visualization and integrated discovery
GO	Gene Ontology
GFAP	Glial fibrillary acidic protein
BMP4	Bone morphogenetic protein 4

S. Obayashi · H. Tabunoki · J.-i. Satoh (✉)
Department of Bioinformatics and Molecular Neuropathology, Meiji Pharmaceutical University, 2-522-1 Noshio, Kiyose, Tokyo 204-8588, Japan
e-mail: satoj@my-pharm.ac.jp

S. U. Kim
Division of Neurology, Department of Medicine, University of British Columbia Hospital, University of British Columbia, Vancouver, BC, Canada

Introduction

Neural stem cells (NSC) with self-renewal and multipotent properties are distributed broadly in the niche of germinal zones in the embryonic and adult mammalian central nervous system (CNS). NSC, unlimitedly propagated in vitro and genetically manipulated ex vivo, could provide an ideal cell source for transplantation to compensate for cell damage in spinal cord injury, stroke, and neurodegenerative diseases (Martino and Pluchino 2006). However, the majority of transplanted NSC and neural progenitor cells (NPC), the cells committed to differentiation into the neuronal lineage, differentiate into astrocytes in vivo under pathological environments in the CNS, which contribute to glial scar formation that inhibits axonal regeneration (Pallini et al. 2005; Ishii et al. 2006). Oxidative stress mediators abundant in pathological lesions elevate the expression of histone deacethylase (HDAC) Sirt1 in mouse NPC, which cooperates with an inhibitory basic helix-loop-helix (bHLH) protein HES1 to mediate epigenetic silencing of a proneural bHLH transcription factor MASH1, leading to astrocyte differentiation of NPC (Prozorovski et al. 2008). To obtain a subset of neurons desirable for cell replacement therapy for human neurological diseases, we should intensively clarify the complex interaction of intrinsic genetic programs and environmental factors that regulate human NSC and NPC proliferation and differentiation. However, at present, molecular mechanisms underlying astrocytic differentiation of human NSC and NPC in vitro and in vivo remain largely unknown.

DNA microarray technology is a powerful approach that allows us to systematically monitor gene expression profile of neural cells during differentiation under development. Microarray analysis showed that neuronal differentiation of human NSC in culture involves the regulation of hundreds of genes, including those essential for Wnt and TGF-beta signaling pathways (Cai et al. 2006). By comparing gene expression profiles between human NPC and differentiated neurons, a previous study identified both PDGF receptor alpha (PDGFRA) and IGF-binding protein 4 (IGFBP4) as key proneural differentiation factors (Yu et al. 2006). A recent study discovered 38 genes expressed commonly between adult and fetal human NPC (Maisel et al. 2007). Recently, we have characterized the DNA damage-responsive gene signature of human astrocytes in culture (Satoh et al. 2006).

Because the serum is a potent inducer of astrocyte differentiation of rodent NSC and NPC in culture (Chiang et al. 1996; Brunet et al. 2004), and the serum components enter the CNS via the disrupted blood–brain barrier (BBB) at the site of CNS injury and ischemia, we studied the effect of the serum on gene expression profile of human NPC in culture by analyzing with a whole genome-scale microarray to identify the gene signature of astrocyte differentiation of human NPC.

Methods

Neural Progenitor Cells in Culture

Cryopreserved human NPC, isolated from the brain of an 18.5-week-old female Caucasian under informed consent, were obtained from Cambrex (Walkersville, MD, USA) as a commercially available product (CC-2599). NPC were plated in a 6-well culture plate coated with polyethyleneimine, and incubated at 37°C in a 5% CO_2/95% air incubator in the NPC medium, composed of the serum-free DMEM/F-12 medium (Invitrogen, Carlsbad, CA, USA) supplemented with a mixture of insulin–transferrin–selenium (ITS) (Invitrogen), 20 ng/ml recombinant human EGF (Higeta, Tokyo, Japan), 20 ng/ml recombinant human bFGF (PeproTech EC, London, UK), and 10 ng/ml recombinant human LIF (Chemicon, Temecula, CA, USA), according to the methods described previously (Carpenter et al. 1999). The half of the medium was renewed every 4 days. Following incubation for several months, NPC in culture continued to proliferate by forming free floating or loosely attached growing spheres. For microarray analysis, nonpassage NPC spheres were harvested, replated in a non-coated 6-well culture plate, and incubated further for 72 h in the NPC medium with or without inclusion of 10% fetal bovine serum (FBS) (Biowest, Miami, FL, USA). In some experiments, NPC were incubated for 72 h in the NPC medium with or without inclusion of 50 ng/ml recombinant human BMP4 (PeproTech).

Human cell lines, such as NTera2 teratocarcinoma, Y79 retinoblastoma, SK-N-SH neuroblastoma, IMR-32 neuroblastoma, U-373MG astrocytoma, HMO6 microglia, HeLa cervical carcinoma, and HepG2 hepatoblastoma, were maintained as described previously (Satoh et al. 2007).

Gene Expression Profiling

Five micrograms of total RNA was isolated from NPC cells by using TRIZOL reagent (Invitrogen). It was in vitro amplified once, and cRNA was processed for microarray analysis on a Whole Human Genome Oligonucleotide Microarray (G4112A, 41,000 genes; Agilent Technologies, Palo Alto, CA, USA), as described previously (Satoh et al. 2006). cRNA prepared from NPC spheres without exposure to the serum (S−) was labeled with a fluorescent dye Cy3, while cRNA of NPC spheres with exposure to the serum (S+) was labeled with Cy5. The array was hybridized at

60°C for 17 h in the hybridization buffer containing equal amounts of Cy3- or Cy5-labeled cRNA. Then, it was scanned by the Agilent scanner (Agilent Technologies). The data were analyzed by using the Feature Extraction software (Agilent Technologies). The fluorescence intensities (FI) of individual spots were quantified following global normalization between Cy3 and Cy5 signals and subsequent Lowess normalization. The ratio of FI of Cy5 signal versus FI of Cy3 signal exceeding 2.0 was defined as significant upregulation, whereas the ratio smaller than 0.5 was considered as substantial downregulation.

Real-Time RT-PCR Analysis

DNase-treated total cellular RNA was processed for cDNA synthesis using oligo(dT)$_{12-18}$ primers and SuperScript II reverse transcriptase (Invitrogen). Then, cDNA was amplified by PCR in LightCycler ST300 (Roche Diagnostics, Tokyo, Japan) using SYBR Green I and primer sets listed in Table 1. The expression levels of target genes were standardized against those of the glyceraldehyde-3-phosphate dehydrogenase (G3PDH) gene detected in parallel in identical cDNA samples. All the assays were performed in triplicate.

Functional Annotation and Molecular Network Analysis

Functional annotation of significant genes identified by microarray analysis was searched by the web-accessible program named Database for Annotation, Visualization and Integrated Discovery (DAVID) version 2008, National Institute of Allergy and Infectious Diseases (NIAID), National Institutes of Health (NIH) (david.abcc.ncifcrf.gov) (Dennis et al. 2003). DAVID covers more than 40 annotation categories, including Gene Ontology (GO) terms, protein–protein interactions, protein functional domains, disease associations, biological pathways, sequence general features, homologies, gene functional summaries, and tissue expressions. By importing the list of the National Center for Biotechnology Information (NCBI) Entrez Gene IDs, this program creates the functional annotation chart, an annotation-term-focused view that lists annotation terms and their associated genes under study. To avoid excessive count of duplicated genes, the Fisher's exact test is calculated based on corresponding DAVID gene IDs by which all redundancies in original IDs are removed.

KeyMolnet is a knowledge-based content database that focuses on relationships among human genes, molecules, diseases, pathways and drugs, which were manually curated by expert biologists (www.immd.co.jp/en/keymolnet/index.html) (Sato et al. 2005). They are categorized into the core contents collected from selected review articles with the highest reliability or the secondary contents extracted from abstracts of PubMed database. The "N-points to N-points" network-search algorithm identifies the molecular network constructed by the shortest route connecting the start point molecules and the end point molecules. The generated network was compared side by side with 346 human canonical pathways of the KeyMolnet library. The algorithm counting the number of overlapping molecular relations between the extracted network and the canonical pathway makes it possible to identify the canonical pathway showing the statistically significant contribution to the extracted network.

Immunohistochemistry

For immunocytochemistry, NPC attached on poly-L-lysine-coated cover glasses were fixed with 4% PFA in 0.1 M phosphate buffer, pH 7.4 at room temperature (RT) for 5 min, followed by incubation with phosphate-buffered saline (PBS) containing 0.5% Triton X-100 at RT for 3 min. After blocking non-specific staining by PBS containing 10% NGS, the cells were incubated at RT for 30 min with a mixture of mouse monoclonal anti-GFAP antibody (GA5; Nichirei, Tokyo, Japan) and rabbit polyclonal anti-nestin antibody (AB5922; Chemicon) or rabbit polyclonal anti-ID1 antibody (C-20; Santa Cruz Biotechnology, Santa Cruz, CA, USA). Then, they were incubated at RT for 30 min with a mixture of Alexa Fluor 488-conjugated anti-rabbit IgG (Invitrogen) and Alexa Fluor 568-conjugated anti-mouse IgG (Invitrogen). After several washes, they were examined on the Olympus BX51 universal microscope.

Western Blot Analysis

To prepare total protein extract, the cells were homogenized in RIPA buffer containing and a cocktail of protease inhibitors (Sigma, St. Louis, MO, USA). Following centrifugation at 12,000 rpm for 10 min at RT, the supernatant was collected and separated on a 12% or 15% SDS–PAGE gel. After gel electrophoresis, the protein was transferred onto nitrocellulose membranes, and the blots were labeled at RT overnight with anti-GFAP antibody (GA5) or anti-ID1 antibody (C-20). Then, they were incubated at RT for 30 min with HRP-conjugated anti-mouse or rabbit IgG (Santa Cruz Biotechnology). The specific reaction was visualized by exposing to a chemiluminescence substrate (Pierce, Rockford, IL, USA). After the antibodies were stripped by incubating the membranes at 50°C for 30 min in stripping buffer, composed of 62.5 mM Tris-HCl, pH 6.7, 2% SDS and 100 mM 2-mercaptoethanol, the blots were processed for relabeling with anti-HSP60 antibody (N-20; Santa Cruz Biotechnology).

Table 1 Primers for PCR for RT-PCR and cloning utilized in the present study

Genes	GenBank accession No.	Sense primers	Antisense primers	Application
NES	NM_006617	5′ctgctcaggagcagcactcttaac3′	5′cttagcctatgagatggagcaggc3′	Real-time RT-PCR
MSI1	NM_002442	5′caaagtgtctatctgggtgtgggc3′	5′acagctgaggcctgcaagcttaca3′	Real-time RT-PCR
GFAP	NM_002055	5′atgaggaggaaggagagaagggga3′	5′ccttccctttcctgtctgagtctc3′	Real-time RT-PCR
NFH	NM_021076	5′gagaaaggaacatccggaacagcc3′	5′tgggagtgccctctcttgctaaca3′	RT-PCR
MBP	NM_002385	5′gttccggaatcctgtcctcagctt3′	5′taactgttggccggaaattgccgg3′	RT-PCR
ID1	NM_002165	5′aattacgtgctctgtgggtctccc3′	5′gtctctggtgactagtaggtgtgc3′	Real-time RT-PCR
ID1	NM_002165	5′atcatggaagtcgccagtggcagc3′	5′tcagcgacacaagatgcgatcgtc3′	Cloning for luciferase assay
Myc-tagged ID1	NM_002165	5′cggaattccgaaagtcgccagtggcagcac3′	5′gaagatcttctcagcgacacaagatgcgat3′	Cloning for CoIP assay
ID3	NM_002167	5′aacttcgccctgcccacttgactt3′	5′cacctccacgctctgaaaagacct3′	Real-time RT-PCR
NPTX1	NM_002522	5′ttgtcctcatgcacacgaagcagc3′	5′acacgcacacacagatcctctcac3′	Real-time RT-PCR
FOS	NM_005252	5′gagctggtgcattacagagaggag3′	5′ggacttgagtccacacatggatgc3′	Real-time RT-PCR
DLL1	NM_005618	5′acgaatgctgctgaagaggaggga3′	5′aactgtccatagtgcaacggcgac3′	Real-time RT-PCR
MASH1	NM_004316	5′tgagtaaggtggagacactgcgct3′	5′tcagaaccagttggtgaagtcgagaag3′	Real-time RT-PCR
Flag-tagged MASH1	NM_002165	5′cggaattccgaaagctctgccaagatggag3′	5′cgggatcccgtcagaaccagttggtgaagt3′	Cloning for CoIP assay and luciferase assay
G3PDH	NM_002046	5′ccatgttcgtcatgggtgtgaacca3′	5′gccagtagaggcagggatgatgttc3′	Real-time RT-PCR
DLL promoter #1	AF222310	5′ggggtaccccctcctgacactaggtggcaaga3′	5′gaagatcttcctcggcctccctccgcctggt3′	Cloning for luciferase assay
DLL promoter #2	AF222310	5′ccgctcgagcggaccccctcggctgccgccgcgg3′	5′gaagatcttccggacagcgcggcggcggcgac3′	Cloning for luciferase assay

NES nestin, *MSI1* musashi homolog 1, *GFAP* glial fibrillary acidic protein, *NFH* neurofilament heavy polypeptide, *MBP* myelin basic protein, *ID1* inhibitor of DNA binding 1, *ID3* inhibitor of DNA binding 3, *NPTX1* neuronal pentraxin 1, *FOS* cellular oncogene c-fos, *DLL1* delta-like 1, *MASH1* mammalian achaete scute homolog 1, *G3PDH* glyceraldehyde-3-phosphate dehydrogenase, *CoIP* coimmunoprecipitation. The underlined sequences represent restriction enzyme sites

Coimmunoprecipitation Analysis

The open-reading frame (ORF) of the human ID1 and MASH1 (ASCL1) genes were amplified by PCR using PfuTurbo DNA polymerase (Stratagene, La Jolla, CA, USA) and primer sets listed in Table 1. They were then cloned into the mammalian expression vector pCMV-Myc (Clontech, Mountain View, CA, USA) or p3XFLAG-CMV7.1 (Sigma) to express a fusion protein with an N-terminal Myc or Flag tag. At 48 h after co-transfection of the vectors in HEK293 cells by Lipofectamine 2000 reagent (Invitrogen), the cells were homogenized in M-PER lysis buffer (Pierce) supplemented with a cocktail of protease inhibitors (Sigma). After preclearance, the supernatant was incubated at 4°C for 3 h with rabbit polyclonal anti-Myc-conjugated agarose (Sigma), mouse monoclonal anti-Flag M2 affinity gel (Sigma), or the same amount of normal mouse or rabbit IgG-conjugated agarose (Santa Cruz Biotechnology). After several washes, the immunoprecipitates were processed for Western blot analysis using rabbit polyclonal anti-Myc antibody (Sigma) and mouse monoclonal anti-FLAG M2 antibody (Sigma).

Dual Luciferase Assay

The ORF of the human ID1 gene, amplified by PCR using PfuTurbo DNA polymerase and primer sets listed in Table 1, was cloned into the mammalian expression vector pEF6/V5-His TOPO (Invitrogen) by designing omission of V5 and His tags. The web search on Database of Transcriptional Start Sites (DBTSS; dbtss.hgc.jp) indicated that several E-box (CANNTG) sequences were clustered in the approximately 3,000 bp promoter region of the human DLL1 gene. Two non-overlapping regions of the DLL1 promoter, consisting of the region #1 spanning −1,253 and −254 containing two E-box sequences or the region #2 spanning −2,946 and −1,786 containing 10 E-box sequences, when the first amino acid of the initiation codon is defined as the position zero, were separately amplified by PCR using GC-RICH PCR system (Roche Diagnostics) and primer sets listed in Table 1. They were then cloned into the Firefly luciferase reporter vector pGL4.14-luc2-Hygro (Promega, Madison, WI, USA). The Renilla luciferase reporter vector pGL4.74-hRluc-TK (Promega) was used for an internal control that normalizes variability caused by differences in transfection efficacy. They were co-transfected in HEK293 cells, which were introduced with MASH1 and/or ID1 expression vectors at 36 h before transfection of the luciferase reporter vectors. At 16 h after transfection of the luciferase reporter vectors, cell lysate was processed for dual luciferase assay on a 20/20 Luminometer (Promega). All the assays were performed in triplicate.

Results

Human Neural Progenitor Cells (NPC) in Culture

Human NPC were capable of proliferating for several months by forming free floating or loosely attached growing spheres, when incubated in the NPC medium under the serum-free culture conditions (Fig. 1a). When human NPC spheres were incubated in the NPC medium supplemented with 10% FBS, they rapidly attached on the plastic surface, followed by vigorous outgrowth of a sheet of adherent cells from the attachment face (Fig. 1b). By RT-PCR analysis, NPC cells expressed the transcripts of nestin (NES), musashi homolog 1 (MSI1), and GFAP at high levels, whereas they displayed fairly low levels of NFH and MBP mRNA under culture conditions with or without inclusion of the serum (Fig. 1c, lanes 1–10).

When incubated in the serum-free NPC medium, the great majority of the cells forming the core of NPC spheres exhibited an intense immunoreactivity for nestin, and expressed less intensely immunoreactivity for GFAP (Fig. 2a). In contrast, when incubated in the 10% FBS-containing NPC medium, virtually all of adherent cells with a polygonal shape, growing out from the NPC spheres, expressed very strongly both GFAP and nestin immunoreactivities (Fig. 2b and d–f). None of the cells expressed the oligodendrocyte marker O4 or O1 in the serum-free and serum-containing culture conditions (data not shown). These results suggest that adherent cells growing from NPC spheres at the attachment face represent the cells that underwent astrocyte differentiation.

Upregulated Genes in Human NPC Following Exposure to the Serum

NPC spheres were harvested, replated on a non-coated plastic surface, and incubated further for 72 h in the NPC medium with (S+) or without (S−) inclusion of 10% FBS. Then, total cellular RNA was processed for microarray analysis. Exposure of NPC spheres to the serum elevated the levels of expression of 45 genes (Table 2). They include tropomodulin 1 (TMOD1), inhibitor of DNA binding 1 (ID1), connective tissue growth factor (CTGF), Kruppel-like factor 9 (KLF9), inhibitor of DNA binding 3 (ID3), fibroblast growth factor binding protein 2 (FGFBP2), zinc finger protein 436 (ZNF436), transforming growth factor alpha (TGFA), tumor protein D52 (TPD52), sulfatase 1 (SULF1), regulator of G-protein signaling 4 (RGS4), collectin sub-family member 12 (COLEC12), angiotensinogen (AGT), solute carrier family 16, member 9 (SLC16A9), meteorin (METRN), cathepsin H (CTSH), growth arrest and DNA-damage-inducible beta (GADD 45B), sterile alpha motif domain containing 11 (SAMD11),

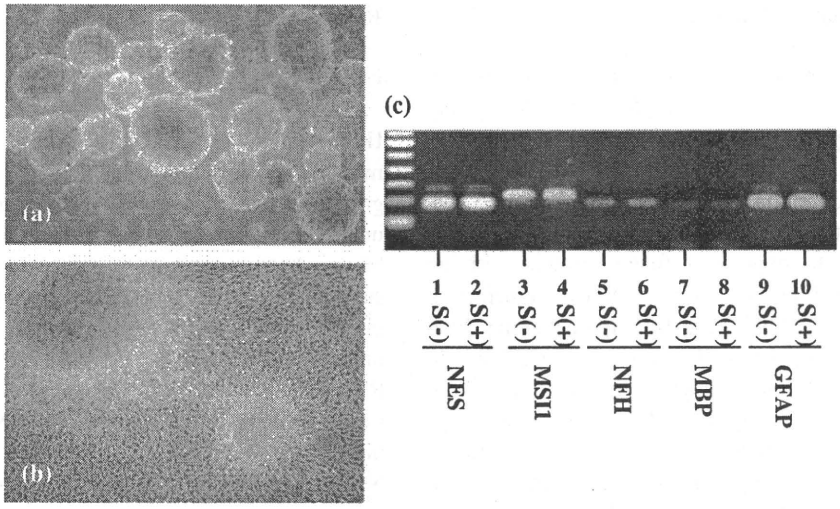

Fig. 1 Human neural progenitor cells (NPC) in culture. **a** Human NPC maintained under the serum-free culture conditions formed free floating growing spheres. **b** Human NPC spheres exposed to 10% FBS rapidly attached on the plastic surface, followed by vigorous outgrowth of a sheet of adherent cells from the attachment face. **a**, **b** Phase-contrast photomicrographs. **c** RT-PCR amplified for 32 cycles of nestin (NES, lanes 1 and 2), musashi homolog 1 (MSI1, lanes 3 and 4), neurofilament heavy polypeptide (NFH, lanes 4 and 6), myelin basic protein (MBP, lanes 7 and 8), and glial fibrillary acidic protein (GFAP, lanes 9 and 10) expressed in human NPC under the serum-free (S−) and the 10% FBS-containing (S+) culture conditions

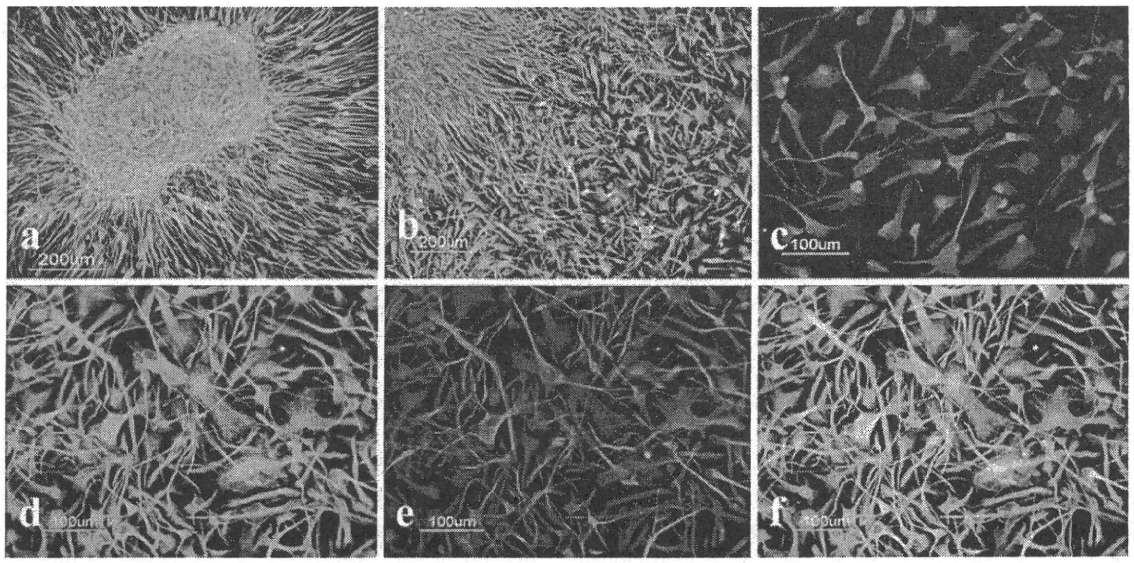

Fig. 2 Nestin, GFAP, and ID1 expression in human NPC in culture. Human NPC spheres attached on poly-L-lysine-coated cover glasses were incubated for 72 h in the NPC medium with (S+) or without (S−) inclusion of 10% FBS, and processed for double-labeling immunocytochemistry for nestin, GFAP, or ID1. **a** S−, NPC sphere, merge of nestin (green) and GFAP (red), **b** S+, vigorous outgrowth of adherent cells from the attachment face of the sphere, merge of nestin (green) and GFAP (red), **c** S+, outgrowth of adherent cells, merge of ID1 (green) and GFAP (red), **d** S+, outgrowth of adherent cells, nestin (green), **e** the same field as **d**, GFAP (red), and **f** merge of **d** and **e**

adenomatosis polyposis coli 2 (APC2), solute carrier family 2 member 5 (SLC2A5), GFAP, coiled-coil domain containing 103 (CCDC103), chromosome 9 open reading frame 58 (C9orf58), chitinase 3-like 2 (CHI3L2), complement factor I (CFI), chemokine C-X-C motif ligand 14 (CXCL14), annexin A1 (ANXA1), regulator of calcineurin 1 (RCAN1), retinal pigment epithelium-specific protein 65 kDa (RPE65), serine/threonine kinase 17a (STK17A), chromosome 4 open reading frame 30 (C4orf30), alpha B crystallin (CRYAB), transmembrane protein 132B (TMEM132B), frizzled homolog 1 (FZD1), inhibitor of DNA binding 2 (ID2), CDC42 effector protein 4

Table 2 Upregulated genes in human neuronal progenitor cells (NPC) following exposure to the serum

Rank	Gene symbol	Gene ID	Ratio	Gene name	Putative function
1	TMOD1	7111	13.05	Tropomodulin 1	A modulator of association between tropomyosin and the spectrin-actin complex
2	ID1	3397	9.00	Inhibitor of DNA binding 1, dominant negative helix-loop-helix protein	A HLH protein that acts as a dominant negative regulator of bHLH family transcription factors
3	CTGF	1490	5.17	Connective tissue growth factor	A secreted mitogenic protein with insulin-like growth factor-binding capacity
4	KLF9	687	4.43	Kruppel-like factor 9	A transcription factor that binds to GC box elements
5	ID3	3399	4.08	Inhibitor of DNA binding 3, dominant negative helix-loop-helix protein	A HLH protein that acts as a dominant negative regulator of bHLH family transcription factors
6	FGFBP2	83888	3.76	Fibroblast growth factor binding protein 2	A protein of unknown function secreted by T lymphocytes
7	ZNF436	80818	3.67	Zinc finger protein 436	A trancriptional factor that represses transcriptional activities of SRE and AP-1
8	TGFA	7039	3.60	Transforming growth factor, alpha	A growth factor that competes with EGF for binding to EGF receptor
9	TPD52	7163	3.35	Tumor protein D52	A coiled-coil domain bearing protein involved in calcium-mediated signal transduction and cell proliferation
10	SULF1	23213	3.23	Sulfatase 1	An endosulfatase that modulates signaling by heparin-binding growth factors
11	RGS4	5999	3.13	Regulator of G-protein signaling 4	A member of RGS family that deactivates G protein subunits of heterotrimeric G proteins
12	COLEC12	81035	2.93	Collectin sub-family member 12	A C-lectin family protein that acts as a scavenger receptor binding to carbohydrate antigens
13	AGT	183	2.90	Angiotensinogen (serpin peptidase inhibitor, clade A, member 8)	Angiotensinogen cleaved by renin to produce angiotensin I
14	SLC16A9	220963	2.82	Solute carrier family 16, member 9 (monocarboxylic acid transporter 9)	A monocarboxylic acid transporter
15	METRN	79006	2.79	Meteorin, glial cell differentiation regulator	A glial cell differentiation regulator
16	CTSH	1512	2.75	Cathepsin H	A lysosomal cysteine proteinase
17	GADD45B	4616	2.70	Growth arrest and DNA-damage-inducible, beta	An environmental stress-inducible protein that activates p38/JNK signaling
18	SAMD11	148398	2.69	Sterile alpha motif domain containing 11	A protein with a SAM motif of unknown function
19	APC2	10297	2.67	Adenomatosis polyposis coli 2	A negative regulator of Wnt signaling
20	SLC2A5	6518	2.63	Solute carrier family 2 (facilitated glucose/fructose transporter), member 5	Glucose/fructose transporter GLUT5
21	GFAP	2670	2.62	Glial fibrillary acidic protein	An intermediate filament protein of astrocytes
22	CCDC103	388389	2.59	Coiled-coil domain containing 103	A coiled-coil domain bearing protein of unknown function
23	C9orf58	83543	2.55	Chromosome 9 open reading frame 58 (ionized calcium binding adapter molecule 2; IBA2)	A calcium binding protein of unknown function
24	CHI3L2	1117	2.52	Chitinase 3-like 2	A secreted chitinase-like protein of unknown function
25	CFI	3426	2.46	Complement factor I	A proteolytic enzyme that inactivates cell-bound, activated C3

Table 2 continued

Rank	Gene symbol	Gene ID	Ratio	Gene name	Putative function
26	CXCL14	9547	2.45	Chemokine (C-X-C motif) ligand 14	A chemoattractant for monocytes and dendritic cells
27	ANXA1	301	2.30	Annexin A1	An annexin family protein with phospholipase A2 inhibitory activity
28	RCAN1	1827	2.29	Regulator of calcineurin 1	A negative regulator of calcineurin signaling
29	RPE65	6121	2.24	Retinal pigment epithelium-specific protein 65 kDa	A protein abundant in retinal pigment epithlium cells involved in the 11-cis retinol synthesis
30	STK17A	9263	2.22	Serine/threonine kinase 17a (apoptosis-inducing)	DAP kinase-related apoptosis-inducing protein kinase DRAK1
31	C4orf30	54876	2.22	Chromosome 4 open reading frame 30 C4orf30	Hypothetical protein LOC27146
32	CRYAB	1410	2.21	Crystallin, alpha B	A small HSP family protein
33	TMEM132B	114795	2.11	Transmembrane protein 132B	A transmembrane protein of unknown function
34	FZD1	8321	2.10	Frizzled homolog 1	A fizzled gene family protein that acts as a receptor for Wnt
35	ID2	3398	2.10	Inhibitor of DNA binding 2, dominant negative helix-loop-helix protein	A HLH protein that acts as a dominant negative regulator of bHLH family transcription factors
36	CDC42EP4	23580	2.09	CDC42 effector protein (Rho GTPase binding) 4	A CDC42-binding protein that interacts with Rho family GTPases
37	NCAN	1463	2.08	Neurocan	Chondroitin sulfate proteoglycan 3 involved in modulation of cell adhesion and migration
38	NAV2	89797	2.07	Neuron navigator 2	A helicase regulated by all-trans retinoic acid that plays a role in neuronal development
39	ENOX1	55068	2.06	Ecto-NOX disulfide-thiol exchanger 1	An enzymes with a hydroquinone (NADH) oxidase activity and a protein disulfide-thiol interchange activity
40	CLSTN2	64084	2.06	Calsyntenin 2	A postsynaptic membrane protein with Ca^{2+}-binding activity
41	NMB	4828	2.03	Neuromedin B	An amidated bombesin-like decapeptide
42	PCSK5	5125	2.02	Proprotein convertase subtilisin/kexin type 5	A member of the subtilisin-like proprotein convertase family
43	MAN1C1	57134	2.02	Mannosidase, alpha, class 1C, member 1	Alpha-1,2-mannosidase IC involved in N-glycan biosynthesis
44	GRAMD1C	54762	2.02	GRAM domain containing 1C	A protein with a GRAM motif of unknown function
45	VAT1	10493	2.01	Vesicle amine transport protein 1	An integral membrane protein of cholinergic synaptic vesicles involved in vesicular transport

Whole Human Genome Microarray (41,000 genes) was hybridized with Cy5-labeled cRNA of NPC incubated in the 10% FBS-containing culture medium and Cy3-labeled cRNA of NPC incubated in the serum-free culture medium. Upregulated genes in NPC by exposure to the serum are listed in order of greatness of the Cy5/Cy3 signal intensity ratio. The results of ID1, ID3, and GFAP (underlined) were validated by real-time RT-PCR analysis (see Fig. 3)

(CDC42EP4), neurocan (NCAN), neuron navigator 2 (NAV2), ecto-NOX disulfide-thiol exchanger 1 (ENOX1), calsyntenin 2 (CLSTN2), neuromedin B (NMB), proprotein convertase subtilisin/kexin type 5 (PCSK5), mannosidase alpha class 1C member 1 (MAN1C1), GRAM domain containing 1C (GRAMD1C), and vesicle amine transport protein 1 (VAT1).

It is worthy to note that three members of ID family genes, ID1, ID2, and ID3, were upregulated coordinately in the serum-treated NPC spheres. The ID family proteins that have an HLH domain but lack the DNA binding domain act as a dominant negative regulator of bHLH transcription factors (Ruzinova and Benezra 2003). Real-time RT-PCR and Western blot analysis validated marked upregulation of ID1, ID3, and GFAP in NPC following exposure to the serum (Fig. 3a–c, g, h). By immunocytochemistry, ID1 was located in the nucleus of GFAP-positive polygonal cells under the serum-containing culture condition

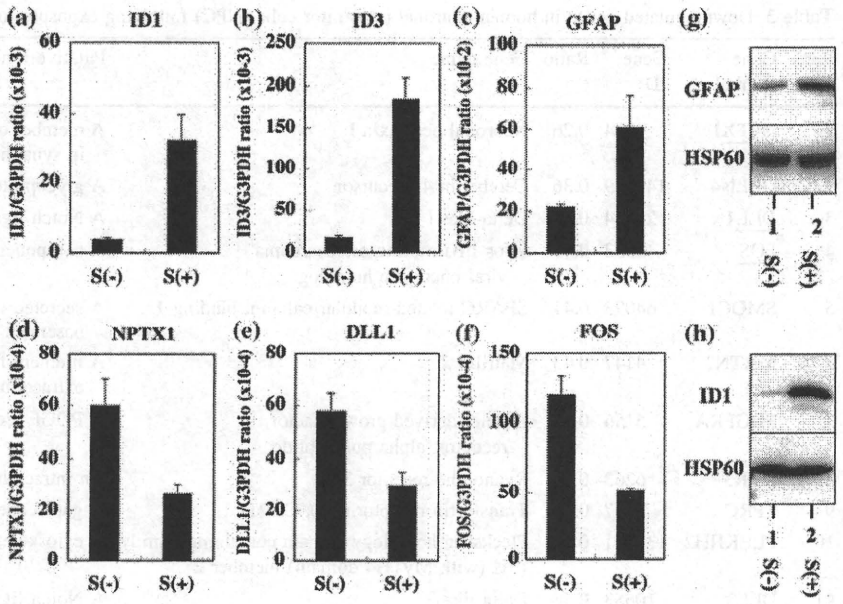

Fig. 3 Validation of microarray data by real-time RT-PCR and western blot analysis. Human NPC spheres were incubated for 72 h in the NPC medium with (S+) or without (S−) inclusion of 10% FBS, and then total cellular RNA or protein extract was processed for real-time RT-PCR and western blot analysis. **a–f** Real-time RT-PCR. The levels of target genes were standardized against the levels of the G3PDH gene. **a** ID1, **b** ID3, **c** GFAP, **d** NPTX1, **e** DLL1, and **f** FOS. **g**, **h** Western blot. The blots were reprobed with anti-HSP60 antibody to serve HSP60 for an internal control. **g** GFAP and **h** ID1

(Fig. 2c). Because GFAP is a defining marker of astrocytes, the results of microarray, RT-PCR, and Western blot verified that the serum promotes astrocyte differentiation of NPC.

Downregulated Genes in Human NPC Following Exposure to the Serum

Exposure of NPC to the serum reduced the levels of expression of 23 genes (Table 3). They include neuronal pentraxin I (NPTX1), cerebellin 4 (CBLN4), delta-like 1 (DLL1), cellular oncogene c-fos (FOS), SPARC related modular calcium binding 1 (SMOC1), matrilin 2 (MATN2), platelet-derived growth factor receptor alpha (PDGFRA), ryanodine receptor 3 (RYR3), transferrin receptor (TFRC), pleckstrin homology domain containing family H member 2 (PLEKHH2), delta-like 3 (DLL3), SRY-box 4 (SOX4), myosin VC (MYO5C), protocadherin 8 (PCDH8), ankyrin repeat domain 10 (ANKRD10), glutamate receptor ionotropic kainate 1 (GRIK1), chondroitin sulfate proteoglycan 4 (CSPG4), cystatin C (CST3), secreted frizzled-related protein 1 (SERP1), ryanodine receptor 1 (RYR1), growth arrest-specific 1 (GAS1), cystatin D (CST5), and hairy and enhancer of split 5 (HES5).

It is worthy to note that the list of downregulated genes included two Notch ligand Delta family members, DLL1 and DLL3, and a Notch effector HES5. It is well known that Notch signaling regulates cell fate specification and multipotency of NSC and NPC (Yoshimatsu et al. 2006). Real-time RT-PCR analysis validated substantial downregulation of NPTX1, DLL1, and FOS in the serum-treated NPC (Fig. 2d–f).

Functional Annotation of the Serum-Responsive Genes in Human NPC

To investigate the functional annotation of the serum-responsive genes in human NPC identified by microarray analysis, the list of Entrez Gene IDs of 45 serum-upregulated genes and 23 serum-downregulated genes was uploaded onto the DAVID database. Top 5 most significant biological processes relevant to the panel of these genes consisted of developmental process (GO:0032502; 32 genes; *P*-value = 2.0E-9), anatomical structure development (GO:0048856; 26 genes; *P*-value = 4.2E-9), multicellular organismal development (GO:0007275; 26 genes; *P*-value = 2.5E-8), system development (GO:0048 731; 20 genes; *P*-value = 2.2E–6), and anatomical structure morphogenesis (GO:0009653; 16 genes; *P*-value = 3.2E–6). The genes involved in the category GO:0032502 include the serum-upregulated genes such as IDI, ID2, ID3, CTGF, TGFA, METRN, KLF9, SULF1, AGT, GADD45B, ANXA1, RCAN1, RPE65, STK17A, CRYAB, FZD1, CDC42EP4, and VAT1, and the serum-downregulated genes such as DLL1, DLL3, HES5, NPTX1, FOS, PDGFRA, RYR1, RYR3, SOX4, PCDH8, GRIK1, CSPG4, SERP1, and GAS1. Thus, the genes whose expression levels were drastically changed in NPC by exposure to the serum are clustered in GO functional categories termed "development."

ID1 Acts as a Negative Regulator of DLL1 Expression

Since the serum-induced astrocyte differentiation of human NPC was followed by remarkable upregulation of ID1, ID2,

Table 3 Downregulated genes in human neuronal progenitor cells (NPC) following exposure to the serum

Rank	Gene symbol	Gene ID	Ratio	Gene name	Putative function
1	NPTX1	4884	0.26	Neuronal pentraxin I	A member of the neuronal pentraxin gene family involved in synaptic plasticity
2	CBLN4	140689	0.36	Cerebellin 4 precursor	A glycoprotein with sequence similarity to precerebellin
3	DLL1	28514	0.38	Delta-like 1	A Notch ligand involved in intercellular communication
4	FOS	2353	0.39	v-fos FBJ murine osteosarcoma viral oncogene homolog	A component of the AP-1 transcription factor complex
5	SMOC1	64093	0.41	SPARC related modular calcium binding 1	A secreted modular calcium-binding glycoprotein in basement membrane
6	MATN2	4147	0.43	Matrilin 2	A filament-forming protein widely distributed in extracellular matrices
7	PDGFRA	5156	0.44	Platelet-derived growth factor receptor, alpha polypeptide	A PDGF receptor component
8	RYR3	6263	0.44	Ryanodine receptor 3	An intracellular calcium release channel
9	TFRC	7037	0.44	Transferrin receptor (p90, CD71)	A gatekeeper for regulating iron
10	PLEKHH2	130271	0.45	Pleckstrin homology domain containing, family H (with MyTH4 domain) member 2	A cytoskeletal protein involved in cell growth
11	DLL3	10683	0.46	Delta-like 3	A Notch ligand involved in intercellular communication
12	SOX4	6659	0.46	SRY (sex determining region Y)-box 4	A member of the SOX family transcription factor involved in the regulation of embryonic development
13	MYO5C	55930	0.46	Myosin VC	A myosin superfamily protein involved in transferrin trafficking
14	PCDH8	5100	0.47	Protocadherin 8	A member of the protocadherin gene family involved in cell adhesion
15	ANKRD10	55608	0.48	Ankyrin repeat domain 10	A protein with ankyrin repeats of unknown function
16	GRIK1	2897	0.48	Glutamate receptor, ionotropic, kainate 1	Ionotropic glutamate receptor subunit GluR5
17	CSPG4	1464	0.48	Chondroitin sulfate proteoglycan 4 (melanoma-associated; NG2)	Chondroitin sulfate proteoglycan that plays a role in stabilizing cell-substratum interaction
18	CST3	1471	0.48	Cystatin C (amyloid angiopathy and cerebral hemorrhage)	An extracellular inhibitor of cycteine proteases
19	SFRP1	6422	0.49	Secreted frizzled-related protein 1	A soluble inhibitor for Wnt signaling
20	RYR1	6261	0.49	Ryanodine receptor 1 (skeletal)	A calcium release channel of the sarcoplasmic reticulum
21	GAS1	2619	0.49	Growth arrest-specific 1	A GPI-anchored protein expressed at growth arrest
22	CST5	1473	0.50	Cystatin D	An extracellular inhibitor of cysteine proteases
23	HES5	388585	0.50	Hairy and Enhancer of split 5 (Drosophila)	bHLH transcription factor downstream of Notch signaling

Whole Human Genome Microarray (41,000 genes) was hybridized with Cy5-labeled cRNA of NPC incubated in the 10% FBS-containing culture medium and Cy3-labeled cRNA of NPC incubated in the serum-free culture medium. Downregulated genes in NPC by exposure to the serum are listed in order of smallness of the Cy5/Cy3 signal intensity ratio. The results of NPTX1, DLL1, and FOS (underlined) were validated by real-time RT-PCR analysis (see Fig. 3)

and ID3, and concomitant downregulation of DLL1 and DLL3, we studied the possible inverse relationship between ID family and Delta family genes with respect to regulation of gene expression. First, by real-time RT-PCR, we determined the levels of ID1 and DLL1 expression in various human neural and non-neural cell lines. The levels of ID1 expression are high but those of DLL1 are very low in HMO6, and HeLa, HepG2, U-373MG, and SK-N-SH, whereas the levels of DLL1 expression are high but those of ID1 are much lower in NTera2 N and IMR-32 (Fig. 4a, b).

Next, we investigated the molecular network of ID1, ID2, ID3, DLL1, and DLL3 by KeyMolnet, a bioinformatics tool for analyzing molecular interaction on the curated knowledge database. The "N-points to N-points" search of KeyMolnet illustrated the shortest route connecting the start point molecules of ID1, ID2, and ID3 and the end point molecules DLL1 and DLL3 (Fig. 5). The pathway based on the molecules showed a significant relationship with canonical pathways of KeyMolnet library, such as transcriptional regulation by SMAD (P-value = 6.6E–12), transcriptional regulation by CREB (P-value = 7.8E–11), and Notch signaling pathway (P-value = 9.7E–9). Although no direct interaction was identified between ID family and Delta family genes,

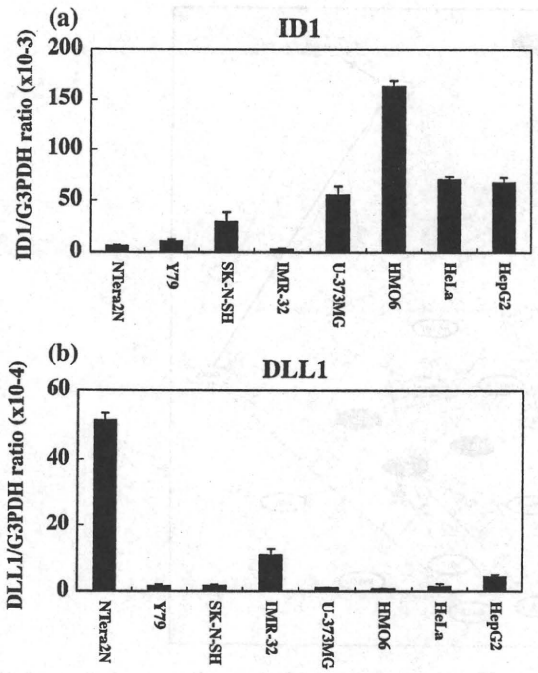

Fig. 4 ID1 and DLL1 expression in various human cell lines. Total RNA of human cell lines, such as NTera2 teratocarcinoma, Y79 retinoblastoma, SK-N-SH neuroblastoma, IMR-32 neuroblastoma, U-373MG astrocytoma, HMO6 microglia, HeLa cervical carcinoma, and HepG2 hepatoblastoma was processed for real-time RT-PCR analysis. The levels of target genes were standardized against the levels of the G3PDH gene. **a** ID1 and **b** DLL1

KeyMolnet indicated two proneural bHLH genes, such as human achaete-scute homolog 1 (HASH1, also known as MASH1 or ASCL) and neurogenin 3 (NGN3, NEUROG3), both of which have an indirect connection with ID1, ID2 and ID3 via HES1, and a T-box gene family member TBX18 as principal regulators of DLL1 expression (Fig. 5). Because microarray analysis indicated that MASH1 is expressed in NPC spheres at much higher levels than NGN3 (data not shown), we confined our attention to a role of MASH1 in the counterbalance between ID and Delta family genes in regulation of gene expression.

Next, we studied the molecular interaction between ID1 and MASH1. By immunoprecipitation analysis of recombinant ID1 and MASH1 proteins coexpressed in HEK293 cells, we identified a direct interaction between ID1 and MASH1 (Fig. 6a, b, lane 2). Then, we cloned two non-overlapping sequences of the human DLL1 promoter containing several E-box sequences, consisting of the region #1 spanning −1,253 and −254 or the region #2 spanning −2,946 and −1,786, in the luciferase reporter vector. Dual luciferase assay indicated that both DLL1 promoter sequences were activated by the expression of MASH1, but this activation was suppressed by the coexpression of ID1 (Fig. 6c, d).

BMP4 Upregulates ID1 and GFAP Expression in Human NPC

Previous studies showed that the serum contains substantial amounts of BMP4 (Kodaira et al. 2006). Because the serum-induced astrocyte differentiation of human NPC was followed by robust upregulation of ID1, we studied the direct effect of BMP4 on expression of ID1 and GFAP in human NPC. When incubated under the serum-free NPC medium, a 72 h-treatment of NPC with 50 ng/ml BMP4 greatly elevated the levels of ID1 and GFAP mRNA expression, suggesting that BMP4 serves as a candidate for astrocyte-inducing factors included in the serum (Fig. 7a, b).

Discussion

We studied the effect of the serum on gene expression profile of cultured human NPC to identify the gene signature of the astrocyte differentiation of human NPC. Following exposure to the serum, human NPC spheres rapidly attached on the plastic surface, and subsequently, adherent cells were differentiated into astrocytes, accompanied by upregulation of GFAP expression, consistent with the previous studies on the rodent NSC and NPC (Chiang et al. 1996; Brunet et al. 2004). The serum elevated the levels of expression of 45 genes in human NPC, including three ID family members ID1, ID2, and ID3, all of which are direct target genes regulated by bone morphogenetic proteins (BMP) (Hollnagel et al. 1999). In contrast, the serum reduced the expression of 23 genes in human NPC, including three Delta-Notch signaling components DLL1, DLL3, and HES5. ID proteins act as a dominant negative regulator of bHLH transcription factors by binding to the ubiquitously expressed bHLH E proteins, such as E2A gene products E12 and E47, or by binding to the cell lineage-restricted bHLH transcription factors (Langlands et al. 1997; Nakashima et al. 2001). By *in silico* molecular network analysis of ID1, ID2, ID3, DLL1, and DLL3 on KeyMolnet, we identified MASH1 as one of important regulators of DLL1 expression. Furthermore, by coimmunoprecipitation analysis, we identified ID1 as a direct binding partner of MASH1. By luciferase assay, we found that activation of DLL1 promoter by MASH1 was counteracted by ID1. Finally, we found that BMP4 elevated the levels of ID1 and GFAP expression in NPC under the serum-free culture conditions. Because the serum contains substantial amounts of BMP4 (Kodaira et al. 2006), our observations raise the possible scenario that the serum factor(s), most probably BMP4, induces astrocyte differentiation by upregulating the expression of ID family genes that repress the proneural bHLH protein-mediated Delta expression in human NPC (Fig. 8).

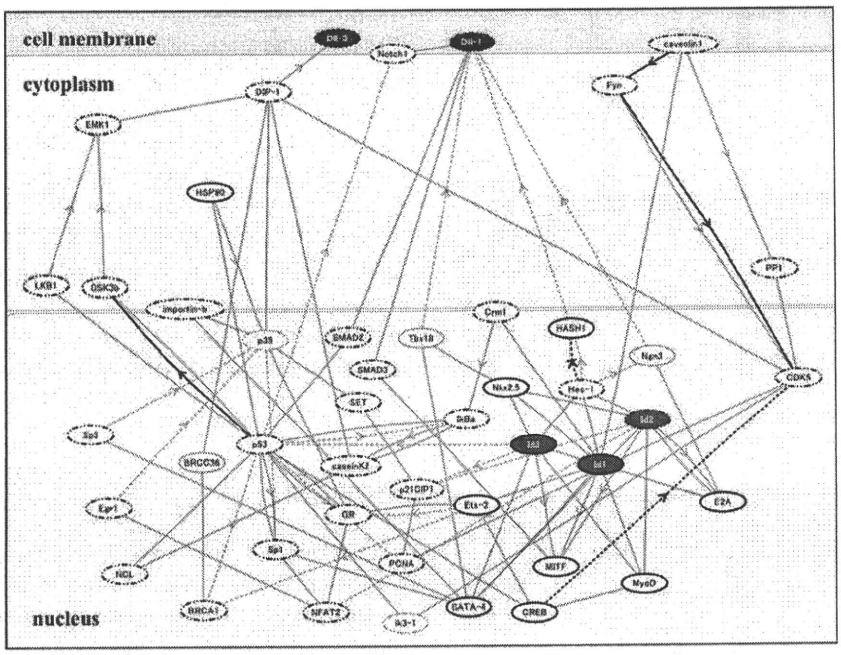

Fig. 5 Molecular network analysis of ID1, ID2, ID3, DLL1, and DLL3. KeyMolnet, a bioinformatics tool for analyzing molecular interaction on the curated knowledge database, identified the shortest route connecting the start point molecules of ID1, ID2, and ID3 (red) and the end point molecules DLL1 and DLL3 (blue). The pathway based on the molecules showed a significant relationship with transcriptional regulation by SMAD or CREB and Notch signaling pathway. The molecular network indicated HASH1 (MASH1), neurogenin 3 (NGN3), and TBX18 as principal regulators of DLL1 expression. The molecular relation is shown by solid line with arrow (direct binding or activation), solid line without arrow (complex formation), and dash line with arrow (transcriptional activation), and dash line with arrow and stop (transcriptional repression). Thick lines indicate the core contents, while thin lines indicate the secondary contents of KeyMolnet

The Serum-Induced Astrocyte Differentiation of Human NPC is Characterized by a Counteraction of ID Family Genes on Delta Family Genes

We proposed the hypothesis that ID genes act as a key positive regulator of the serum-induced astrocyte differentiation of human NPC. The following previous observations support this view. The expression of four ID members is transiently elevated in immortalized mouse astrocyte precursor cells during astrocyte differentiation (Andres-Barquin et al. 1997). ID gene expression is rapidly induced in cultured rat astrocytes following stimulation with the serum (Tzeng and de Vellis 1997). Treatment of rodent NPC with BMP4 induces the expression of four ID genes, followed by induction of astrocyte differentiation, while the complex formation of ID4 or ID2 with bHLH proteins OLIG1 and OLIG2 blocks oligodendrocyte lineage commitment (Samanta and Kessler 2004).

ID proteins also act as a negative regulator of neuronal differentiation by preventing premature exit of neuroblasts from the cell cycle (Lyden et al. 1999). Retroviral vector-mediated overexpression of ID1 in the mouse brain in vivo inhibits neurogenesis but promotes astrocytogenesis (Cai et al. 2000). BMP2 induces the expression of ID1 and ID3, which inhibit the transcriptional activity of MASH1 and E47 complex on an E-box-containing promoter, suggesting that ID protein-mediated antagonism of proneural bHLH transcription factors plays a role in inhibition of neuronal differentiation (Nakashima et al. 2001). Combinatorial actions of proneural bHLH and inhibitory HLH factors regulate the timing of differentiation of NPC (Kageyama et al. 2005). ID1 binds not only to E proteins but also to myogenic bHLH transcription factors MYOD and MYF5 with high affinity (Langlands et al. 1997). We found that ID1 is a direct binding partner of neurogenic bHLH transcription factor MASH1. MASH1 deficient mice showed a severe loss of NPC in the subventricular zone of the medial ganglionic eminence, and MASH1, expressed in NPC, regulates neuronal differentiation by inducing the expression of Notch ligands DLL1 and DLL3, resulting in activation of Notch signaling in adjacent cells (Casarosa et al. 1999; Ito et al. 2000). Importantly, Mash1 directly activates the promoter of DLL1 gene (Castro et al. 2006). The activation of Delta-Notch signaling plays a key role in maintenance of NPC in the undifferentiated state (Yoshimatsu et al. 2006).

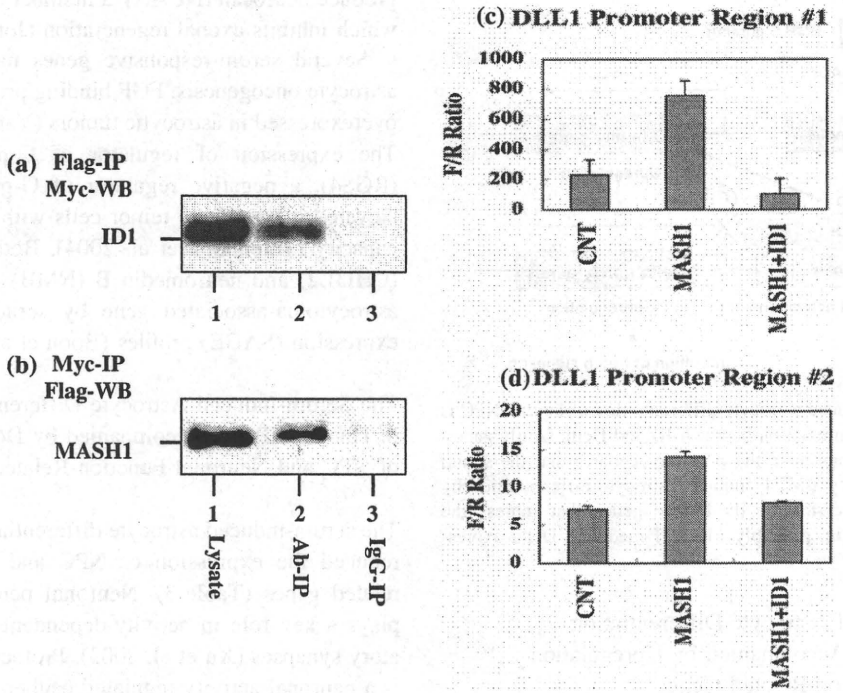

Fig. 6 Activation of the DLL1 promoter by MASH1 was counteracted by ID1. **a**, **b** Coimmunoprecipitation analysis. Recombinant MASH1 protein tagged with Flag and ID1 protein tagged with Myc were coexpressed in HEK293 cells. Immunoprecipitation (IP) followed by Western blotting (WB) was performed by using the antibodies against Flag and Myc. The lanes (1–3) represent (1) input control of cell lysate, (2) IP with anti-Flag or anti-Myc antibody, and (3) IP with normal mouse or rabbit IgG. **c**, **d** Dual luciferase assay. Two non-overlapping regions of the human DLL1 promoter, consisting of the region #1 spanning −1,253 and −254 or the region #2 spanning −2,946 and −1,786, were cloned into the Firefly luciferase reporter vector. It was co-transfected with the Renilla luciferase reporter vector (an internal control) in HEK293 cells, which were introduced with none (CNT), MASH1, or both MASH1 and ID1 expression vectors at 36 h before transfection of the luciferase reporter vectors. At 16 h after transfection of the luciferase reporter vectors, cell lysate was processed for dual luciferase assay. The ratio of Firefly (F)/Renilla (R) luminescence (RLU) is indicated

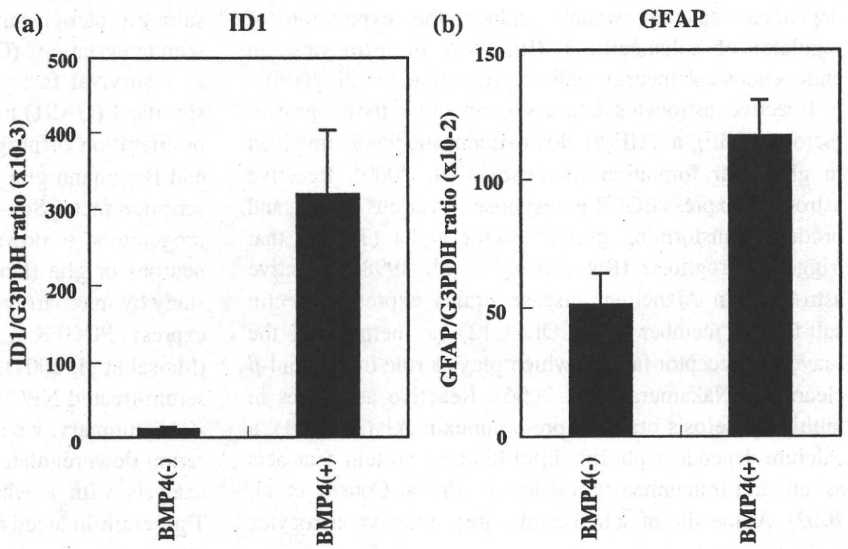

Fig. 7 BMP4 upregulates ID1 and GFAP expression in human NPC. Human NPC were incubated for 72 h in the NPC medium with (+) or without (−) inclusion of 50 ng/ml recombinant human BMP4, and then total cellular RNA was processed for real-time RT-PCR analysis. The levels of target genes were standardized against the levels of the G3PDH gene. **a** ID1 and **b** GFAP

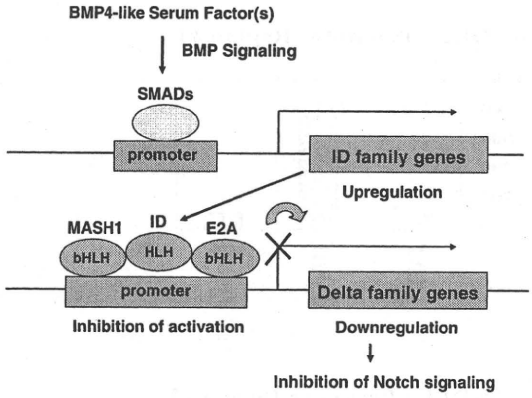

Fig. 8 The serum-induced astrocyte differentiation of human NPC is characterized by a counteraction between ID and Delta family genes. The present observations raise the possible scenario that the serum factor(s), most probably BMP4, induces astrocyte differentiation by upregulating the expression of ID family genes that repress the proneural bHLH protein, probably MASH1-mediated Delta expression in human NPC

The Serum-Induced Astrocyte Differentiation of Human NPC is Accompanied by Upregulation of Astrocyte Function-Related Genes

The serum-induced astrocyte differentiation of human NPC elevated the expression of astrocyte function-related genes (Table 2). Astrocytes express angiotensinogen (AGT) that plays a role in maintenance of the blood–brain barrier (BBB) function (Kakinuma et al. 1998). Astrocytes synthesize cathepsin H (CTSH) that acts as a metabolizing enzyme for neuropeptides and bradykinin (Brguljan et al. 2003). Human astrocytes in culture express complement factor I (CFI) essential for regulating the complement cascade (Gordon et al. 1992). Neuronal and glial progenitor cells secrete meterorin (METRN) that stimulates astrocyte differentiation in culture (Nishino et al. 2004). Calcineurin-dependent calcium signals induce the expression of regulator of calcineurin 1 (RCAN1) in astrocytes, an endogenous calcineurin inhibitor (Canellada et al. 2008).

Reactive astrocytes express connective tissue growth factor (CTGF), a TGF-β1 downstream mediator, involved in glial scar formation (Schwab et al. 2000). Reactive astrocytes express EGFR in response to various insults, and produce transforming growth factor alpha (TGFA) that triggers astrogliosis (Rabchevsky et al. 1998). Reactive astrocytes in Alzheimer disease brains express collectin sub-family member 12 (COLEC12), a member of the scavenger receptor family, which plays a role in amyloid-β clearance (Nakamura et al. 2006). Reactive astrocytes in multiple sclerosis brains express annexin A1 (ANXA1), a calcium-dependent phospholipid-binding protein that acts as an anti-inflammatory mediator (Probst-Cousin et al. 2002). At the site of spinal cord injury, reactive astrocytes produce neurocan (NCAN), a member of the CSPG family, which inhibits axonal regeneration (Jones et al. 2003).

Several serum-responsive genes have implications in astrocyte oncogenesis. FGF binding protein 2 (FGFBP2) is overexpressed in astrocytic tumors (Yamanaka et al. 2006). The expression of regulator of G-protein signaling 4 (RGS4), a negative regulator of G-protein signaling, is elevated in astrocytic tumor cells with a highly migratory capacity (Tatenhorst et al. 2004). Both chitinase 3-like 2 (CHI3L2) and neuromedin B (NMB) are identified as an astrocytoma-associated gene by serial analysis of gene expression (SAGE) profiles (Boon et al. 2004).

The Serum-Induced Astrocyte Differentiation of Human NPC is Accompanied by Downregulation of NPC and Neuronal Function-Related Genes

The serum-induced astrocyte differentiation of human NPC reduced the expression of NPC and neuronal function-related genes (Table 3). Neuronal pentaraxin I (NPTX1) plays a key role in activity-dependent plasticity of excitatory synapses (Xu et al. 2003). Protocadherin 8 (PCDH8) is a neuronal activity-regulated cadherin involved in long-term potentiation in the hippocampus (Yamagata et al. 1999). Spinal cord motor neurons express the ionotropic kainite receptor subunit GRIK1 (GluR5) (Eubanks et al. 1993). Ryanodine receptors RyR1, RyR2, and RyR3 are intracellular calcium release channels expressed in subpopulations of neurons in the human CNS (Martin et al. 1998).

NPC expressing the PDGF α-receptor (PDGFRA) proliferate in response to PDGF-AA associated with induction of c-fos (FOS) expression (Erlandsson et al. 2001). NPC express the transferrin receptor (TFRC, CD71) (Sergent-Tanguy et al. 2006), while oligodendrocyte progenitor cells express NG2 (CSPG4), an integral membrane chondroitin sulfate proteoglycan (Chang et al. 2000). NSC and NPC secrete cystatin C (CST3) into the culture medium, serving as a survival factor (Taupin et al. 2000). Growth arrest-specific 1 (GAS1) induced by Wnt signaling is required for proliferation of progenitors of the cerebellar granule cells and Bergmann glia (Liu et al. 2001). The HMG-box transcription factor Sox4, expressed in neuronal as well as glial progenitors, is downregulated in terminally differentiated neurons or glia (Hoser et al. 2007). Importantly, a recent study by microarray analysis showed that fetal human NPC express PDGFRA, CSPG4, DLL3, GAS1, and SOX4 (Maisel et al. 2007), all of which are downregulated in the serum-treated NPC in the present study.

In summary, we identified 45 serum-upregulated and 23 serum-downregulated genes in human NPC in culture by analysis with a whole human genome-scale microarray. The serum-induced astrocyte differentiation of human NPC

is characterized by a counteraction of ID family genes on Delta family genes.

Acknowledgments This work was supported by a research Grant to J-IS from the High-Tech Research Center Project, the Ministry of Education, Culture, Sports, Science and Technology (MEXT), Japan (S0801043).

References

Andres-Barquin PJ, Hernandez MC, Hayes TE, McKay RD, Israel MA (1997) Id genes encoding inhibitors of transcription are expressed during in vitro astrocyte differentiation and in cell lines derived from astrocytic tumors. Cancer Res 57:215–220

Boon K, Edwards JB, Eberhart CG, Riggins GJ (2004) Identification of astrocytoma associated genes including cell surface markers. BMC Cancer 4:39. doi:10.1186/1471-2407-4-39

Brguljan PM, Turk V, Nina C, Brzin J, Krizaj I, Popovic T (2003) Human brain cathepsin H as a neuropeptide and bradykinin metabolizing enzyme. Peptides 24:1977–1984. doi:10.1016/j.peptides.2003.09.018

Brunet JF, Grollimund L, Chatton JY, Lengacher S, Magistretti PJ, Villemure JG, Pellerin L (2004) Early acquisition of typical metabolic features upon differentiation of mouse neural stem cells into astrocytes. Glia 46:8–17. doi:10.1002/glia.10348

Cai L, Morrow EM, Cepko CL (2000) Misexpression of basic helix-loop-helix genes in the murine cerebral cortex affects cell fate choices and neuronal survival. Development 127:3021–3030

Cai Y, Wu P, Ozen M, Yu Y, Wang J, Ittmann M, Liu M (2006) Gene expression profiling and analysis of signaling pathways involved in priming and differentiation of human neural stem cells. Neuroscience 138:133–148. doi:10.1016/j.neuroscience.2005.11.041

Canellada A, Ramirez BG, Minami T, Redondo JM, Cano E (2008) Calcium/calcineurin signaling in primary cortical astrocyte cultures: Rcan1-4 and cyclooxygenase-2 as NFAT target genes. Glia 56:709–722. doi:10.1002/glia.20647

Carpenter MK, Cui X, Hu ZY, Jackson J, Sherman S, Seiger A, Wahlberg LU (1999) In vitro expansion of a multipotent population of human neural progenitor cells. Exp Neurol 158:265–278. doi:10.1006/exnr.1999.7098

Casarosa S, Fode C, Guillemot F (1999) Mash1 regulates neurogenesis in the ventral telencephalon. Development 126:525–534

Castro DS, Skowronska-Krawczyk D, Armant O, Donaldson IJ, Parras C, Hunt C, Critchley JA, Nguyen L, Gossler A, Göttgens B, Matter JM, Guillemot F (2006) Proneural bHLH and Brn proteins coregulate a neurogenic program through cooperative binding to a conserved DNA motif. Dev Cell 11:831–844. doi:10.1016/j.devcel.2006.10.006

Chang A, Nishiyama A, Peterson J, Prineas J, Trapp BD (2000) NG2-positive oligodendrocyte progenitor cells in adult human brain and multiple sclerosis lesions. J Neurosci 20:6404–6412

Chiang YH, Silani V, Zhou FC (1996) Morphological differentiation of astroglial progenitor cells from EGF-responsive neurospheres in response to fetal calf serum, basic fibroblast growth factor, and retinol. Cell Transplant 5:179–189. doi:10.1016/0963-6897(95)02043-8

Dennis G Jr, Sherman BT, Hosack DA, Yang J, Gao W, Lane HC, Lempicki RA (2003) DAVID: database for annotation, visualization, and integrated discovery. Genome Biol 4:R60. doi:10.1186/gb-2003-4-9-r60

Erlandsson A, Enarsson M, Forsberg-Nilsson K (2001) Immature neurons from CNS stem cells proliferate in response to platelet-derived growth factor. J Neurosci 21:3483–3491

Eubanks JH, Puranam RS, Kleckner NW, Bettler B, Heinemann SF, McNamara JO (1993) The gene encoding the glutamate receptor subunit GluR5 is located on human chromosome 21q21.1–22.1 in the vicinity of the gene for familial amyotrophic lateral sclerosis. Proc Natl Acad Sci USA 90:178–182. doi:10.1073/pnas.90.1.178

Gordon DL, Avery VM, Adrian DL, Sadlon TA (1992) Detection of complement protein mRNA in human astrocytes by the polymerase chain reaction. J Neurosci Methods 45:191–197. doi:10.1016/0165-0270(92)90076-P

Hollnagel A, Oehlmann V, Heymer J, Rüther U, Nordheim A (1999) Id genes are direct targets of bone morphogenetic protein induction in embryonic stem cells. J Biol Chem 274:19838–19845. doi:10.1074/jbc.274.28.19838

Hoser M, Baader SL, Bösl MR, Ihmer A, Wegner M, Sock E (2007) Prolonged glial expression of Sox4 in the CNS leads to architectural cerebellar defects and ataxia. J Neurosci 27:5495–5505. doi:10.1523/JNEUROSCI.1384-07.2007

Ishii K, Nakamura M, Dai H, Finn TP, Okano H, Toyama Y, Bregman BS (2006) Neutralization of ciliary neurotrophic factor reduces astrocyte production from transplanted neural stem cells and promotes regeneration of corticospinal tract fibers in spinal cord injury. J Neurosci Res 84:1669–1681. doi:10.1002/jnr.21079

Ito T, Udaka N, Yazawa T, Okudela K, Hayashi H, Sudo T, Guillemot F, Kageyama R, Kitamura H (2000) Basic helix-loop-helix transcription factors regulate the neuroendocrine differentiation of fetal mouse pulmonary epithelium. Development 127:3913–3921

Jones LL, Margolis RU, Tuszynski MH (2003) The chondroitin sulfate proteoglycans neurocan, brevican, phosphacan, and versican are differentially regulated following spinal cord injury. Exp Neurol 182:399–411. doi:10.1016/S0014-4886(03)00087-6

Kageyama R, Ohtsuka T, Hatakeyama J, Ohsawa R (2005) Roles of bHLH genes in neural stem cell differentiation. Exp Cell Res 306:343–348. doi:10.1016/j.yexcr.2005.03.015

Kakinuma Y, Hama H, Sugiyama F, Yagami K, Goto K, Murakami K, Fukamizu A (1998) Impaired blood-brain barrier function in angiotensinogen-deficient mice. Nat Med 4:1078–1080. doi:10.1038/2070

Kodaira K, Imada M, Goto M, Tomoyasu A, Fukuda T, Kamijo R, Suda T, Higashio K, Katagiri T (2006) Purification and identification of a BMP-like factor from bovine serum. Biochem Biophys Res Commun 345:1224–1231. doi:10.1016/j.bbrc.2006.05.045

Langlands K, Yin X, Anand G, Prochownik EV (1997) Differential interactions of Id proteins with basic-helix-loop-helix transcription factors. J Biol Chem 272:19785–19793. doi:10.1074/jbc.272.32.19785

Liu Y, May NR, Fan CM (2001) Growth arrest specific gene 1 is a positive growth regulator for the cerebellum. Dev Biol 236:30–45. doi:10.1006/dbio.2000.0146

Lyden D, Young AZ, Zagzag D, Yan W, Gerald W, O'Reilly R, Bader BL, Hynes RO, Zhuang Y, Manova K, Benezra R (1999) Id1 and Id3 are required for neurogenesis, angiogenesis and vascularization of tumour xenografts. Nature 401:670–677. doi:10.1038/44334

Maisel M, Herr A, Milosevic J, Hermann A, Habisch HJ, Schwarz S, Kirsch M, Antoniadis G, Brenner R, Hallmeyer-Elgner S, Lerche H, Schwarz J, Storch A (2007) Transcription profiling of adult and fetal human neuroprogenitors identifies divergent paths to maintain the neuroprogenitor cell state. Stem Cells 25:1231–1240. doi:10.1634/stemcells.2006-0617

Martin C, Chapman KE, Seckl JR, Ashley RH (1998) Partial cloning and differential expression of ryanodine receptor/calcium-release channel genes in human tissues including the hippocampus and cerebellum. Neuroscience 85:205–216. doi:10.1016/S0306-4522(97)00612-X

Martino G, Pluchino S (2006) The therapeutic potential of neural stem cells. Nat Rev Neurosci 7:395–406. doi:10.1038/nrn1908

Nakamura K, Ohya W, Funakoshi H, Sakaguchi G, Kato A, Takeda M, Kudo T, Nakamura T (2006) Possible role of scavenger receptor SRCL in the clearance of amyloid-β in Alzheimer's disease. J Neurosci Res 84:874–890. doi:10.1002/jnr.20992

Nakashima K, Takizawa T, Ochiai W, Yanagisawa M, Hisatsune T, Nakafuku M, Miyazono K, Kishimoto T, Kageyama R, Taga T (2001) BMP2-mediated alteration in the developmental pathway of fetal mouse brain cells from neurogenesis to astrocytogenesis. Proc Natl Acad Sci USA 98:5868–5873. doi:10.1073/pnas.101109698

Nishino J, Yamashita K, Hashiguchi H, Fujii H, Shimazaki T, Hamada H (2004) Meteorin: a secreted protein that regulates glial cell differentiation and promotes axonal extension. EMBO J 23:1998–2008. doi:10.1038/sj.emboj.7600202

Pallini R, Vitiani LR, Bez A, Casalbore P, Facchiano F, Di Giorgi Gerevini V, Falchetti ML, Fernandez E, Maira G, Peschle C, Parati E (2005) Homologous transplantation of neural stem cells to the injured spinal cord of mice. Neurosurgery 57:1014–1025. doi:10.1227/01.NEU.0000180058.58372.4c

Probst-Cousin S, Kowolik D, Kuchelmeister K, Kayser C, Neundörfer B, Heuss D (2002) Expression of annexin-1 in multiple sclerosis plaques. Neuropathol Appl Neurobiol 28:292–300. doi:10.1046/j.1365-2990.2002.00396.x

Prozorovski T, Schulze-Topphoff U, Glumm R, Baumgart J, Schröter F, Ninnemann O, Siegert E, Bendix I, Brüstle O, Nitsch R, Zipp F, Aktas O (2008) Sirt1 contributes critically to the redox-dependent fate of neural progenitors. Nat Cell Biol 10:385–394. doi:10.1038/ncb1700

Rabchevsky AG, Weinitz JM, Coulpier M, Fages C, Tinel M, Junier MP (1998) A role for transforming growth factor alpha as an inducer of astrogliosis. J Neurosci 18:10541–10552

Ruzinova MB, Benezra R (2003) Id proteins in development, cell cycle and cancer. Trends Cell Biol 13:410–418. doi:10.1016/S0962-8924(03)00147-8

Samanta J, Kessler JA (2004) Interactions between ID and OLIG proteins mediate the inhibitory effects of BMP4 on oligodendroglial differentiation. Development 131:4131–4412. doi:10.1242/dev.01273

Sato H, Ishida S, Toda K, Matsuda R, Hayashi Y, Shigetaka M, Fukuda M, Wakamatsu Y, Itai A (2005) New approaches to mechanism analysis for drug discovery using DNA microarray data combined with KeyMolnet. Curr Drug Discov Technol 2:89–98. doi:10.2174/1570163054064701

Satoh J, Tabunoki H, Nanri Y, Arima K, Yamamura T (2006) Human astrocytes express 14-3-3 sigma in response to oxidative and DNA-damaging stresses. Neurosci Res 56:61–72. doi:10.1016/j.neures.2006.05.007

Satoh J, Tabunoki H, Yamamura T, Arima K, Konno H (2007) TROY and LINGO-1 expression in astrocytes and macrophages/microglia in multiple sclerosis lesions. Neuropathol Appl Neurobiol 33:99–107. doi:10.1111/j.1365-2990.2006.00787.x

Schwab JM, Postler E, Nguyen TD, Mittelbronn M, Meyermann R, Schluesener HJ (2000) Connective tissue growth factor is expressed by a subset of reactive astrocytes in human cerebral infarction. Neuropathol Appl Neurobiol 26:434–440. doi:10.1046/j.1365-2990.2000.00271.x

Sergent-Tanguy S, Véziers J, Bonnamain V, Boudin H, Neveu I, Naveilhan P (2006) Cell surface antigens on rat neural progenitors and characterization of the CD3 (+)/CD3 (−) cell populations. Differentiation 74:530–541. doi:10.1111/j.1432-0436.2006.00098.x

Tatenhorst L, Senner V, Püttmann S, Paulus W (2004) Regulators of G-protein signaling 3 and 4 (RGS3, RGS4) are associated with glioma cell motility. J Neuropathol Exp Neurol 63:210–222

Taupin P, Ray J, Fischer WH, Suhr ST, Hakansson K, Grubb A, Gage FH (2000) FGF-2-responsive neural stem cell proliferation requires CCg, a novel autocrine/paracrine cofactor. Neuron 28:385–397. doi:10.1016/S0896-6273(00)00119-7

Tzeng SF, de Vellis J (1997) Expression and functional role of the Id HLH family in cultured astrocytes. Brain Res Mol Brain Res 46:136–142. doi:10.1016/S0169-328X(96)00294-X

Xu D, Hopf C, Reddy R, Cho RW, Guo L, Lanahan A, Petralia RS, Wenthold RJ, O'Brien RJ, Worley P (2003) Narp and NP1 form heterocomplexes that function in developmental and activity-dependent synaptic plasticity. Neuron 39:513–528. doi:10.1016/S0896-6273(03)00463-X

Yamagata K, Andreasson KI, Sugiura H, Maru E, Dominique M, Irie Y, Miki N, Hayashi Y, Yoshioka M, Kaneko K, Kato H, Worley PF (1999) Arcadlin is a neural activity-regulated cadherin involved in long term potentiation. J Biol Chem 274:19473–19479. doi:10.1074/jbc.274.27.19473

Yamanaka R, Arao T, Yajima N, Tsuchiya N, Homma J, Tanaka R, Sano M, Oide A, Sekijima M, Nishio K (2006) Identification of expressed genes characterizing long-term survival in malignant glioma patients. Oncogene 25:5994–6002. doi:10.1038/sj.onc.1209585

Yoshimatsu T, Kawaguchi D, Oishi K, Takeda K, Akira S, Masuyama N, Gotoh Y (2006) Non-cell-autonomous action of STAT3 in maintenance of neural precursor cells in the mouse neocortex. Development 133:2553–2563. doi:10.1242/dev.02419

Yu S, Zhang JZ, Xu Q (2006) Genes associated with neuronal differentiation of precursors from human brain. Neuroscience 141:817–825. doi:10.1016/j.neuroscience.2006.02.080

Disease Markers 27 (2009) 239–252
DOI 10.3233/DMA-2009-0670
IOS Press

Molecular network analysis suggests aberrant CREB-mediated gene regulation in the Alzheimer disease hippocampus

Jun-ichi Satoh[a,*], Hiroko Tabunoki[a] and Kunimasa Arima[b]
[a]*Department of Bioinformatics and Molecular Neuropathology, Meiji Pharmaceutical University, 2-522-1 Noshio, Kiyose, Tokyo 204-8588, Japan*
[b]*Department of Psychiatry, National Center Hospital, National Center of Neurology and Psychiatry, 4-1-1 Ogawahigashi, Kodaira, Tokyo 187-8551, Japan*

Abstract. The pathogenesis of Alzheimer disease (AD) involves the complex interaction between genetic and environmental factors affecting multiple cellular pathways. Recent advances in systems biology provide a system-level understanding of AD by elucidating the genome-wide molecular interactions. By using KeyMolnet, a bioinformatics tool for analyzing molecular interactions on the curated knowledgebase, we characterized molecular network of 2,883 all stages of AD-related genes (ADGs) and 559 incipient AD-related genes (IADGs) identified by global gene expression profiling of the hippocampal CA1 region of AD brains in terms of significant clinical and pathological correlations (Blalock et al., Proc Natl Acad Sci USA 101: 2173-2178, 2004). By the common upstream search, KeyMolnet identified cAMP-response element-binding protein (CREB) as the principal transcription factor exhibiting the most significant relevance to molecular networks of both ADGs and IADGs. The CREB-regulated transcriptional network included upregulated and downregulated sets of ADGs and IADGs, suggesting an involvement of generalized deregulation of the CREB signaling pathway in the pathophysiology of AD, beginning at the early stage of the disease. To verify the *in silico* observations *in vivo*, we conducted immunohistochemical studies of 11 AD and 13 age-matched control brains by using anti-phoshorylated CREB (pCREB) antibody. An abnormal accumulation of pCREB imunoreactivity was identified in granules of granulovacuolar degeneration (GVD) in the hippocampal neurons of AD brains. These observations suggest that aberrant CREB-mediated gene regulation serves as a molecular biomarker of AD-related pathological processes, and support the hypothesis that sequestration of pCREB in GVD granules is in part responsible for deregulation of CREB-mediated gene expression in AD hippocampus.

Keywords: Alzheimer disease, CREB, granulovacuolar degeneration, keymolnet, molecular network, systems biology

1. Introduction

Alzheimer disease (AD) is the most common cause of dementia worldwide, affecting the elderly population, characterized by the hallmark pathology of amyloid-β (Aβ) deposition and neurofibrillary tangle (NFT) formation in the brain. The complex interaction between genetic and environmental factors affecting multiple cellular pathways plays a role in the pathogenesis of AD [1]. The completion of the Human Genome Project in 2003 allows us to systematically characterize the comprehensive disease-associated profiles of the whole human genome. It promotes us to identify disease-specific and stage-specific molecular signatures and biomarkers for diagnosis and prediction of prognosis, and druggable targets for therapy [2]. Actually, global transcriptome analysis of AD brains identified a battery of genes aberrantly regulated in AD, whose role has not been previously

*Corresponding author: Prof. Dr. Jun-ichi Satoh, Department of Bioinformatics and Molecular Neuropathology, Meiji Pharmaceutical University, 2-522-1 Noshio, Kiyose, Tokyo 204-8588, Japan. Tel./Fax: +81 42 495 8678; E-mail: satoj@my-pharm.ac.jp.

ISSN 0278-0240/09/$17.00

predicted in its pathogenesis. They include reduced expression of kinases/phosphatases, cytoskeletal proteins, synaptic proteins, and neurotransmitter receptors in NFT-bearing CA1 neurons [3], downregulaton of neurotrophic factors and upregulation of proapoptotic molecules in the hippocampal CA1 region [4], disturbed sphingolipid metabolism in various brain regions during progression of AD [5], and overexpression of the AMPA receptor GluR2 subunit in synaptosomes of prefrontal cortex [6]. However, in global expression analysis, the important biological implications are often left behind to be characterized, because the huge amount of high-density microarray data is highly complex. Furthermore, cardinal observations obtained from *in silico* data analysis should be validated by independent wet lab experiments.

Recent advances in systems biology enable us to illustrate a cell-wide map of the complex molecular interactions with aid of the literature-based knowledgebase of molecular pathways [7,8]. In the scale-free molecular network, targeted disruption of several critical components, on which the biologically important molecular connections concentrate, could disturb the whole cellular function by destabilizing the network [9]. Thus, molecular network analysis goes beyond gene-by-gene analysis to shed light on a system-level understanding of molecular relationships among individual genes and networks.

The present study is designed to conduct molecular network analysis of a published microarray dataset of Blalock et al. [10]. It contains genome-wide expression profiling of hippocampal CA1 tissues derived from 22 AD patients with well-defined clinical and pathological stages. They identified 3,413 all stages of AD-related genes (ADGs) and 609 incipient AD-related genes (IADGs), and characterized overrepresented genes by using a bioinformatics tool named Expression Analysis Systematic Explorer (EASE). They found upregulation of tumor suppressors, oligodendrocyte growth factors, and protein kinase A (PKA) modulators, along with downregulation of protein folding/metabolism/transport machinery molecules in incipient AD (IAD) [10]. Recently, a different study followed up analysis of this dataset by weighted gene coexpression network analysis (WGCNA) that calculates a matrix containing all pairwise Pearson correlations between whole microarray probe sets across all subjects in an unsupervised manner. They identified AD-related coexpression modules that play key roles in synaptic transmission, extracellular transport, mitochondrial and metabolic functions, and myelination [11]. However, all of these studies did not clarify the common upstream transcription factors governing molecular networks, closely associated with deregulated gene expression in AD brains. By using KeyMolnet, a bioinformatics tool for analyzing molecular interactions on the curated knowledgebase [12], we characterized the most relevant molecular network of AD brain transcriptome, composed of the genes coordinately regulated by putative common upstream transcription factors.

2. Materials and methods

2.1. The dataset

We performed molecular network analysis of ADGs and IADGs, derived from a dataset of Blalock et al. [10]. It contains gene expression profiling of frozen tissues of the CA1 hippocampus, performed by analyzing with the Affymetrix Human Genome HG-U133A chip that contains 22,215 transcripts. The complete dataset is available from Gene Expression Omnibus (GEO) database (GSE1297). RNA was isolated from the samples of 31 age-matched individuals, composed of nine control subjects, seven patients with incipient AD (IAD), eight with moderate AD, and seven with severe AD [10]. The dataset was normalized following the Microarray Analysis Suite 5.0 (MAS5) algorithm. The clinical stage of AD was defined by the Mini-Mental State Examination (MMSE) score, i.e. control (MMSE $>$ 25), incipient AD (MMSE 20–26), moderate AD (MMSE 14–19), and severe AD (MMSE $<$ 14). The neurofibrillary tangle (NFT) burden was determined in each brain sample, which always showed an inverse relationship with the MMSE score. The statistical correlation between the expression levels of individual genes and the MMSE and NFT scores was evaluated by Pearson's correlation tests and ANOVA. With respect to overall correlations across 31 subjects, the study identified 3,413 ADGs, composed of 1,977 upregulated and 1,436 downregulated genes in all stages of AD patients versus control subjects. The study also identified 609 IADGs, composed of 431 upregulated and 178 downregulated genes in IAD patients versus control subjects.

2.2. Gene ID conversion

We converted Affymetrix probe IDs into the corresponding National Center for Biotechnology Information (NCBI) Entrez Gene IDs by using the

Database for Annotation, Visualization and Integrated Discovery (DAVID) 2008 Gene ID conversion tool (david.abcc.ncifcrf.gov) [13]. Then, we excluded a set of non-annotated genes, overlapping genes, and those listed concurrently in both upregulated and downregulated classes.

2.3. Molecular network analysis

KeyMolnet is a comprehensive knowledgebase, originally developed by the Institute of Medicinal Molecular Design (IMMD), Tokyo, Japan [12]. It covers virtually all the relationships heretofore reported among human genes, molecules, diseases, pathways and drugs, whose information is manually collected, carefully curated, and regularly updated by expert biologists. The database is categorized into the core contents collected from selected review articles with the highest reliability, or the secondary contents extracted from abstracts of PubMed database and Human Protein Reference database (HPRD). By importing microarray data, such as the list of Entrez Gene ID and fold changes of individual probes, KeyMolnet automatically provides corresponding molecules as a node on networks.

The common upstream search is a mode of network analysis that extracts the most relevant molecular network composed of the genes coordinately regulated by putative common upstream transcription factors. The generated network was compared side by side with 403 human canonical pathways of the KeyMolnet library. To reduce the potential bias toward the selection of major pathways, all well-established biological pathways covering both major and minor classes were collected by extensive search of valid review articles with journal impact factors greater than 10. Further information on the canonical pathways of KeyMolnet is available from IMMD upon request (www.immd.co.jp/en/keymolnet/index.html). The algorithm counting the number of overlapping molecular relations between the extracted network and the canonical pathway makes it possible to identify the canonical pathway showing the most significant contribution to the extracted network. It is constructed by modification of the algorithm developed for GO::TermFinder [14]. The significance in the similarity between the extracted network and the canonical pathway is scored following the formula, where O = the number of overlapping molecular relations between the extracted network and the canonical pathway, V = the number of molecular relations located in the extracted network, C = the number of molecular relations located in the canonical pathway, T = the number of total molecular relations composed of approximately 110,000 sets, and the X = the sigma variable that defines coincidence.

$$\text{Score} = -\log_2(\text{Score}(p))$$

$$\text{Score}(p) = \sum_{x=O}^{Min(C,V)} f(x)$$

$$f(x) = {}_C C_x \cdot {}_{T-C} C_{V-x} / {}_T C_V$$

2.4. Immunohistochemistry

The autopsied brain samples were provided by Research Resource Network (RRN), Japan. Written informed consent was obtained form all the cases. The Ethics Committee of National Center of Neurology and Psychiatry approved the present study. The study population consists of 11 AD patients composed of five men and six women with the mean age of 71 ± 9 years, and 13 other neurological disease (termed as non-AD) patients composed of six men and seven women with the mean age of 69 ± 9 years. The non-AD cases include three patients with Parkinson disease (PD), two with multiple system atrophy (MSA), four with amyotrophic lateral sclerosis (ALS), and four with myotonic dystrophy. The average of brain weight was 1,038 ± 163 gram in AD cases and 1,195 ± 182 gram in non-AD cases. Brain tissues of the hippocampus and the motor cortex were fixed with 4% paraformaldehyde (PFA), embedded in paraffin, and processed for ten micron-thick serial sections. All AD cases were satisfied with the Consortium to Establish a Registry for Alzheimer's Disease (CERAD) criteria for diagnosis of definite AD [15]. They were categorized into the stage C of amyloid deposition and the stage VI of neurofibrillary degeneration, following the Braak's staging [16].

The immunohistochemistry protocol was described elsewhere [17]. In brief, after deparaffination, tissue sections were heated in 10 mM citrate sodium buffer, pH 6.0 by autoclave at 125°C for 30 sec in a temperature-controlled pressure chamber (Dako, Tokyo, Japan). They were incubated with 3% hydrogen peroxide-containing methanol to block the endogenous peroxidase activity, and with phosphate-buffered saline (PBS) containing 10% normal goat serum (NGS) at room temperature (RT) for 15 min to block non-specific staining. Then, tissue sections were stained at 4°C overnight with rabbit polyclonal anti-phoshorylated cAMP-response element-binding protein (pCREB) an-